



Adsorption of copper ions on porous ceramsite prepared by diatomite and tungsten residue

Qing-xiu JING^{1,2}, Yun-yan WANG¹, Li-yuan CHAI¹, Chong-jian TANG¹,
Xiao-dong HUANG², Huan GUO², Wei WANG², Wei YOU²

1. School of Metallurgy and Environment, Central South University, Changsha 410083, China;

2. School of Metallurgical and Chemical Engineering,

Jiangxi University of Science and Technology, Ganzhou 341000, China

Received 30 September 2017; accepted 10 January 2018

Abstract: In order to realize resource utilization of industrial tungsten residue and treatment of heavy metal wastewater in mining and metallurgical area of south China, a novel ceramsite was prepared with the main raw materials of diatomite and tungsten residue. The adsorption behavior of copper ions in solution on the ceramsite was investigated. Results indicated that the surface of the newly-developed ceramsite was rough and porous. There were lots of pores across the ceramsite from inner to outside. MnFe_2O_4 was one of the main components of the ceramsite. The Cu^{2+} adsorption capacity by the ceramsite reached 9.421 mg/g with copper removal efficiency of 94.21% at 303 K, initial Cu^{2+} concentration of 100 mg/L and dosage of 0.5 g after 300 min adsorption. With increase of ceramsite dosage, the total adsorption amount of Cu^{2+} increased, but the adsorption capacity decreased. The adsorption capacity increased with the increase of solution pH. The isothermal adsorption of Cu^{2+} by the ceramsite fitted the Freundlich model better. The adsorption mainly occurred on a heterogeneous surface, and was a favorable process. The adsorption process closely followed the pseudo-second kinetic equation. In initial stage of wastewater treatment, the adsorption process should be controlled mainly by diffusion, and the removal of Cu^{2+} can be improved by enhancing agitation.

Key words: tungsten residue; ceramsite; heavy metal wastewater; Cu^{2+} ; adsorption

1 Introduction

Due to its high toxicity, heavy metal in wastewater even at extremely low concentration will cause great harm to the environment [1,2]. In nonferrous mining and metallurgical area of south China, heavy metal wastewater has already caused serious pollution and damage to the ecological environment [3,4]. At present, among those common methods used for treating heavy metal wastewater, adsorption possesses potential application prospect due to the advantages of high efficiency and no selectivity [5,6]. However, the high cost for adsorbent preparation has restricted its wide application.

Ceramsite can be used as an excellent adsorption or filtration material, due to its high porosity, high temperature resistance, strong corrosion resistance,

strong cylinder compressive strength, and so on [7]. Recently, some researches about heavy metal wastewater treated by ceramsite have been reported. WANG et al [8] have investigated the adsorption properties of porous ceramsite from streambed sediments and sludge for Cu^{2+} and Cd^{2+} in wastewater, in which the adsorption capacities of Cu^{2+} and Cd^{2+} could reach 4.96 mg/g and 3.84 mg/L, respectively. JI et al [9] have studied the adsorption performance of ceramsite from fly ash and iron modified agents for ammonia nitrogen and phosphorus. Their results supported the application of ceramsite as a filter media. LIU et al [10] revealed that a ceramsite prepared from sewage sludge had water absorption of 6% and compressive strength of 6.6 MPa, and the ceramsite could be safely used as a light weight aggregate. Accordingly, ceramsite has excellent promising application for purification of heavy metal wastewater.

Foundation item: Project (51674305) supported by the National Natural Science Foundation of China; Key Project (1602FKDC007) supported by Science and Technology Program of Gansu Province, China; Projects (2016YT03N101, 2017A090905024) supported by Science and Technology Program of Guangdong Province, China; Project (NSFJ2015-K06) supported by Jiangxi University of Science and Technology, China

Corresponding author: Chong-jian TANG; Tel: +86-731-88830511; E-mail: chjtang@csu.edu.cn

DOI: 10.1016/S1003-6326(18)64731-4

On the other hand, a large amount of tungsten residue has been produced and it is dumped as solid waste in the great majority of tungsten extracting plants in mining and metallurgical area of south China. The accumulated stock of tungsten waste residue has reached millions of tons [11]. This not only occupies large amount of useful land, but also contaminates environment and wastes resources. These problems are expected to be solved if a ceramsite can be prepared from the tungsten residue. Whereas, tungsten residue contains low silicon, which cannot be cemented to a regular shape by sintering itself alone. Diatomite is a plentiful, cheap and high silicon containing rock powder material. The rich silicon can help to shape the ceramsite at high temperature. So, a new ceramsite is expected to be prepared with the tungsten residue and diatomite.

At present time, the development and utilization of tungsten residue are still less reported due to its difficult disposal, if in the present study, a novel ceramsite can be prepared with tungsten residue and diatomite and can be applied to treating heavy metal wastewater, the reutilization of industrial tungsten residue could be possible. This is of great significance for the tungsten extracting plants, and can provide a new purification method for local heavy metal wastewater treatment. Moreover, a “win-win” effect can be obtained by treating heavy metal wastewater with the nearby tungsten wastes for nonferrous mining and metallurgical areas in south China.

2 Experimental

2.1 Materials

The experimental tungsten residue was provided by a local tungsten metallurgy company. The chemical composition (mass fraction, %) is: Fe_2O_3 30.75, MnO_2 15.65, CaO 7.44, SiO_2 5.99, Al_2O_3 0.61, Na_2O 1.55. No radioactive element exceeding the national standard was detected from the tungsten residue. The diatomite raw material was purchased from Tianjin Fuchen Chemical Reagent Co., Ltd, China. The additives, kaoline and sodium bicarbonate, were purchased from Ganzhou Ganhu reagent Co., Ltd, China. After being crushed and washed, the tungsten residue was dried at 110 °C for 5 h, blending with dried diatomite and additives. Then, the samples were screened through 100 mesh sieve spare. All the experimental reagents were of analytical grade unless otherwise stated.

2.2 Adsorbent preparation

According to a required proportion, the diatomite, tungsten residue, sintering aids and pore forming agent were weighed, and mixed together with a small amount of deionized water. The diameter of the particles was

controlled from 2 to 8 mm. After being dried, the particles were sintered and cooled in sintering furnace.

2.3 Analytical methods for adsorbent

The performance of the ceramsite was measured according to the corresponding national standard. The morphology and structure were observed by a scanning electron microscopy (SEM) typed TM3030. The crystal structure was established by an X-ray diffractometry (XRD) typed Empyrean (Cu target, using the K_α radiation, a wavelength λ of 0.1542 nm and range in angle from 5° to 80°). The sample group structure was analyzed by a Fourier transform infrared spectroscopy (FT-IR) typed ALPHA (with a sample: KBr mass ratio of 1:100). Copper ion concentration was measured by an atomic adsorption spectrophotometer typed TAS-990.

2.4 Adsorption methods

1) A certain amount of synthetic Cu^{2+} -containing wastewater with a required concentration was prepared with CuSO_4 reagent. 50 mL of each solution was measured and transferred into a 100 mL polyethylene bottle with a stopper. Ceramsite was then added into the bottle. After adjusting pH to a certain value, a series of suspensions were then agitated at a set temperature for 5 h. Subsequently, the suspensions were centrifuged and filtered. The concentrations of Cu^{2+} in supernatants at equilibrium, ρ_e , were measured, and the adsorption capacities, Q_e , could be calculated accordingly.

2) 100 mg/L of Cu^{2+} -containing solution was prepared. 50 mL of each solution was measured and transferred into a 100 mL polyethylene bottle. Then, the solution pH was adjusted to a certain value and ceramsites with prepared amount were added into the solution. After several bottles of this suspension were prepared, they were agitated in an oscillating equipment at a set temperature. One of the suspension bottles was taken out for sampling at different time, followed by centrifuging and filtrating. The concentrations of Cu^{2+} in supernatants at contact time t , ρ_t were measured, and the adsorption capacities at contact time t , Q_t , could be calculated accordingly.

During this part, the effects of ceramsite dosage, initial pH of the solution on adsorption were evaluated. The adsorption equilibrium time was also determined. The pseudo-first-order, pseudo-second-order, intra-particle diffusion and Elovich models were adopted to investigate the adsorption kinetics.

3) Isothermal adsorption methods

Copper-containing solutions with different initial concentrations of 20, 40, 50, 60, 80 and 100 mg/L were prepared and 50 mL of each solution was mixed with 0.5 g of ceramsite under 288, 303 and 318 K, respectively. Afterwards, the suspensions were adjusted

to the same pH and agitated at the fixed temperature for 5 h. After the suspensions were centrifuged, separated and filtrated, the values of ρ_e were measured, and Q_e was calculated accordingly. The experimental data were fitted by Langmuir model and Freundlich model, respectively.

3 Results and discussion

3.1 Characteristics of ceramsite

3.1.1 Physicochemical performance of ceramsite

The ceramsite sample was prepared under optimized raw material ratios and sintering techniques. Results showed that the water adsorption, porosity, pulverization ratio, acid dissolution rate and density of the prepared ceramsite were 44.93%, 44.56%, 0.951%, 1.4% and 0.8752 g/cm^3 , respectively, which met the requirements of ceramsite performance for water treating according to the standard of CJ/T 299–2008 [12]. The toxicity of the ceramsite was detected according to standards of HJ/T299–2007 [13] and GB 5085.3–2007 [14]. The leaching results also met the corresponding requirements. Therefore, the ceramsite can be used for wastewater treatment.

3.1.2 SEM images of ceramsite

The SEM images of the ceramsite are presented in Fig. 1. As shown in Fig. 1(a), the shape of the tungsten residue and diatomite-based ceramsite is near spherical with rough and porous surface. There are lots of pores in ceramsite from inner part to the outside (Fig. 1(b)). Hence, the adsorption of Cu^{2+} ions in solution is likely to occur on the ceramsite surface and the internal structure.

3.1.3 XRD pattern of ceramsite

The XRD patterns of the raw tungsten residue and the ceramsite sample are shown in Fig. 2. The main components of tungsten residue are oxides of iron and manganese (Fig. 2(a)), while the main components of the ceramsite contain MnFe_2O_4 (PDF#38–0430), SiO_2 (PDF#82–1564) and CaSiO_3 (PDF#88–1922) (Fig. 2(b)). As MnFe_2O_4 has good adsorption capacity for cationic ions [15], the ceramic would have good removal performance on heavy metal ions-containing wastewater.

3.1.4 FT-IR spectrum of ceramsite

The FT-IR spectrum of the ceramsite is presented in Fig. 3. In Fig. 3, bands at 1000 , 790 and 569 cm^{-1} are caused by the stretching vibration of Si—O—Si , Si—O and Fe—O groups [16–18], respectively. And band at 1650 cm^{-1} is assigned to the —OH bending vibration of water in ceramsite [8].

According to the FT-IR analysis results of the ceramsite, it is clear that the ceramsite contains a large number of Si—O—Si groups and Fe—O polar groups. The latter is especially beneficial to the adsorption removal of Cu^{2+} from solution.

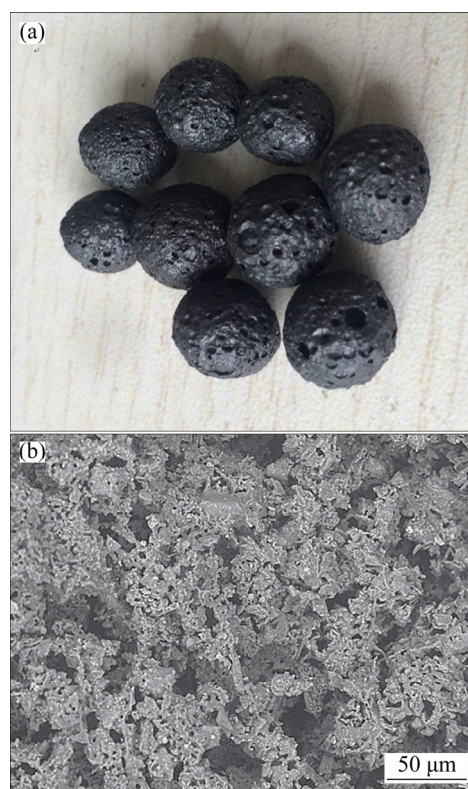


Fig. 1 SEM images of ceramsite sample: (a) Surface morphology; (b) Interior structures

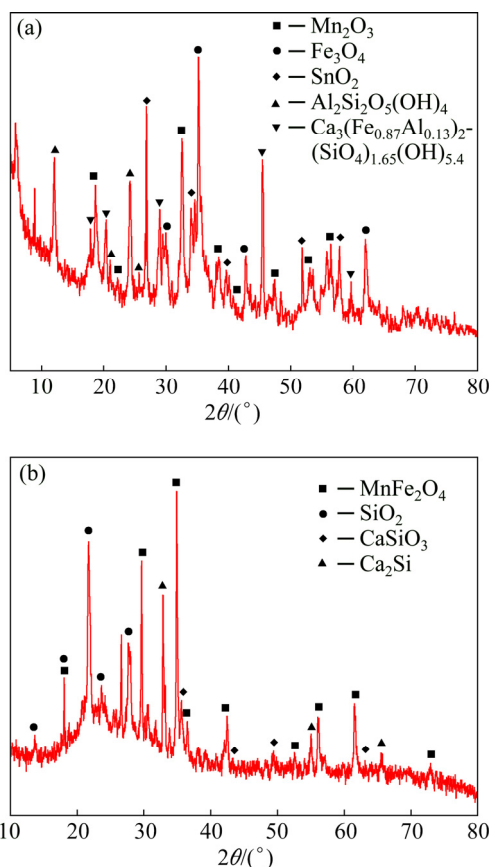


Fig. 2 XRD patterns of tungsten residue (a) and ceramsite sample (b)

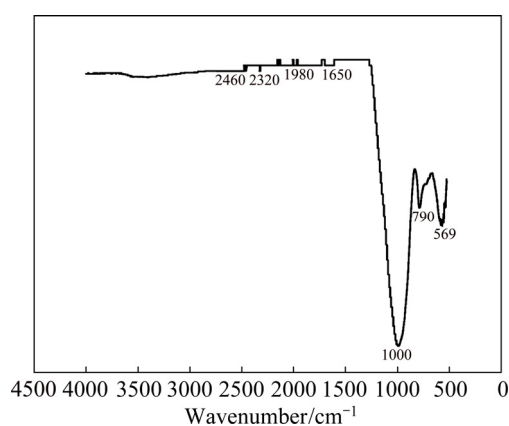


Fig. 3 FT-IR spectrum of ceramsite sample

3.2 Effects of adsorption factors on Cu^{2+} removal by ceramsite

3.2.1 Effect of ceramsite dosage

The effect of ceramsite dosage on Cu^{2+} adsorption was evaluated at 303 K, with ρ_0 of 100 mg/L. The results are shown in Fig. 4. In Fig. 4(a), under the three different ceramsite dosage conditions, the Cu^{2+} concentration tends to maintain stable after about 300 min adsorption, showing that the adsorption reaches equilibrium. With

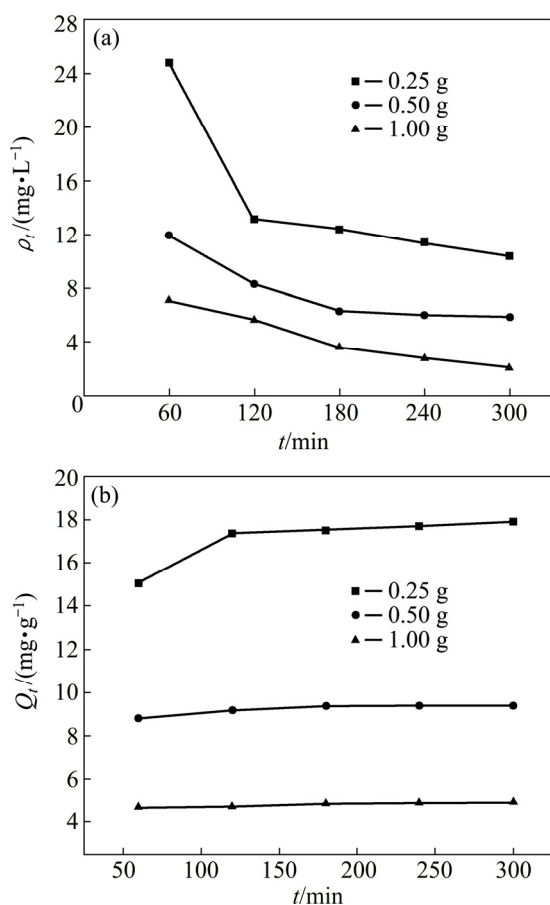


Fig. 4 Effects of ceramsite dosage on Cu^{2+} adsorption by ceramsite ($T=303$ K, $\rho_0=100$ mg/L): (a) Cu^{2+} concentration in solution; (b) Variation of adsorption capacity

the increase of ceramsite dosage, the Cu^{2+} concentration in solution decreases. When the ceramsite dosage reaches 1.0 g, the Cu^{2+} concentration decreases to about 2.0 mg/L after 300 min adsorption. Figure 4(b) shows that the adsorption capacity of Cu^{2+} by the ceramsite decreases with the increasing dosage. With the increase of ceramsite dosage, the adsorption force of specific surface area of the ceramsite for Cu^{2+} is weakened, so the adsorption capacity decreases.

3.2.2 Effect of initial pH of solution

The effect of initial pH of solution on Cu^{2+} adsorption by the ceramsite was evaluated ($T=303$ K, $\rho_0=100$ mg/L, 0.5 g ceramsite) by avoiding hydrolysis reaction of Cu^{2+} in solution. The results are presented in Fig. 5.

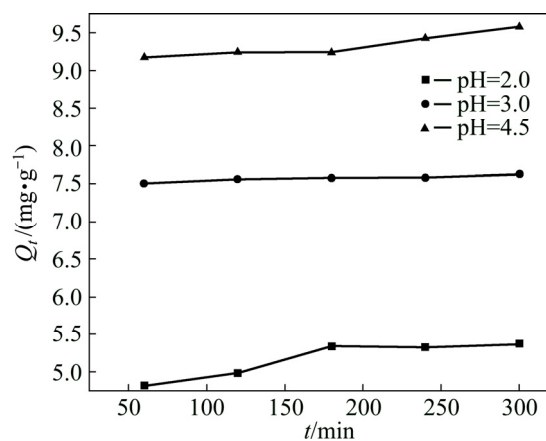


Fig. 5 Effect of initial pH of solution on Cu^{2+} adsorption by ceramsite ($T=303$ K, $\rho_0=100$ mg/L)

As from Fig. 5, the adsorption capacity increases with increase of the initial pH value. The reason is that under the lower pH, the higher H^+ concentration in solution resulting in stronger ion exchange of H^+ with the polar groups of ceramsite. Consequently, numerous adsorption sites could be occupied by H^+ , thus decreasing the adsorption capacity of Cu^{2+} . As the interaction between the ceramsite adsorbent and Cu^{2+} ions relies on the electrostatic interaction between them and the overall surface charge of ceramsite will become more negative when pH is increased [15], the binding force between the ceramsite polar groups and Cu^{2+} ions will be enhanced. Therefore, the overall adsorption capacity will increase with increase of the initial pH of the solution.

3.2.3 Determination of equilibrium adsorption time

The variations of Cu^{2+} concentration (ρ_i) and adsorption capacity (Q_t) along with time (t) were evaluated ($T=303$ K, $\rho_0=100$ mg/L) and shown in Fig. 6.

As from Fig. 6, when t was shorter than 180 min, the Cu^{2+} concentration in solution decreases rapidly with the increase of t (Fig. 6(a)), while the adsorption capacity

increases correspondingly (Fig. 6(b)). When t was shorter than 300 min, the adsorption capacity still increases slowly with increase of t . After 300 min contact, the Cu^{2+} concentration and the adsorption capacity almost remain unchanged, indicating that adsorption reaches equilibrium. Accordingly, the equilibrium adsorption time can be determined as 300 min. At that time, the Cu^{2+} concentration is about 5.79 mg/L, and the adsorption capacity is 9.421 mg/g with Cu^{2+} removal of 94.21%. Thus, in treating Cu^{2+} -containing wastewater with the ceramsite, the removal equilibrium time can be determined as 300 min.

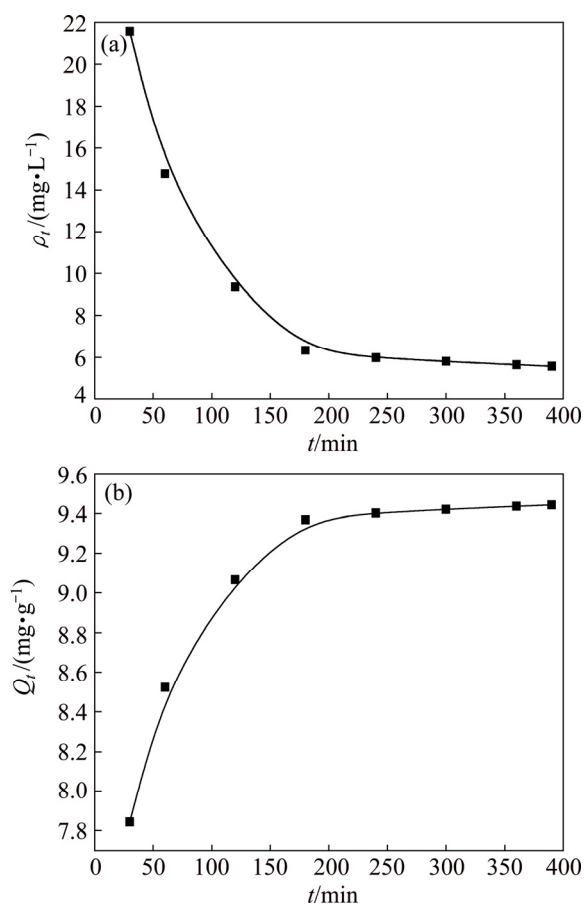


Fig. 6 Relationships between initial Cu^{2+} concentration ρ_i and t (a), and between adsorption capacity Q_t and t (b)

3.3 Isothermal adsorption and kinetics

3.3.1 Isothermal adsorption

In this section, Langmuir and Freundlich adsorption models were used to fit the experimental data, respectively. Langmuir adsorption model is based on the assumption of a monolayer adsorption on a structurally homogeneous adsorbent, where all the sorption sites are identical and energetically equivalent. When the adsorbent surface is saturated, the adsorption capacity reaches a maximum value. The Langmuir isothermal equation is presented as Eq. (1) [19]:

$$\frac{\rho_e}{Q_e} = \frac{1}{K_L Q_m} + \frac{\rho_e}{Q_m} \quad (1)$$

where K_L is the Langmuir constant; Q_m is the theoretical maximum adsorption capacity corresponding to a monolayer coverage.

Freundlich isothermal model is an empirical equation, which is adequate for an adsorbent surface being non-uniform. Its linear form is given by Eq. (2) [20]:

$$\ln Q_e = \ln K_F + 1/n \ln \rho_e \quad (2)$$

where K_F is the Freundlich constant; n is an empirical parameter relating to the adsorption intensity (when the value of $1/n$ lies between 0.1 and 1, the adsorption process is favorable [21]).

The results fitted by Langmuir and Freundlich models are shown in Fig. 7 and Table 1.

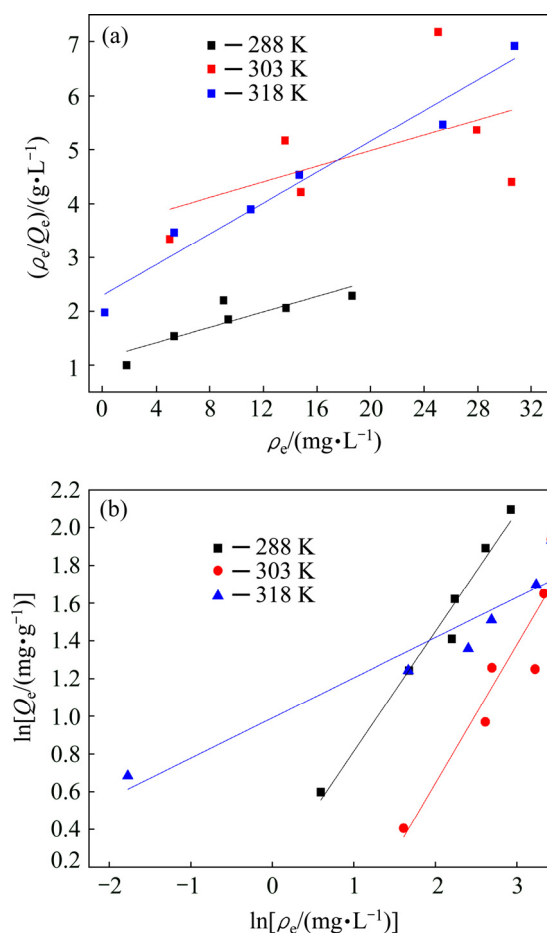


Fig. 7 Linear fitting plots of Cu^{2+} adsorption by porous ceramsite at different temperatures with Langmuir model (a), and Freundlich model (b)

From Fig. 7 and Table 1, the correlation coefficients R^2 for Freundlich model are higher than those of Langmuir model. Moreover, $1/n$ locates in the range of 0–1, indicating that the Cu^{2+} adsorption by ceramsite fits

Freundlich model better. Thus, the adsorption tends to occur on a heterogeneous surface, and the adsorption was a favorable process.

Table 1 Langmuir and Freundlich isotherm parameters for copper ions adsorbed by ceramsite

T/K	Langmuir			Freundlich		
	$Q_m/$ ($\text{mg}\cdot\text{g}^{-1}$)	$K_L/$ ($\text{L}\cdot\text{mg}^{-1}$)	R^2	n	$K_F/$ ($\text{mg}\cdot\text{g}^{-1}$)	R^2
288	14.05	0.0625	0.695	1.576	1.198	0.968
303	13.89	0.0203	0.119	1.357	0.437	0.845
318	7.006	0.0621	0.952	4.965	2.696	0.885

3.3.2 Kinetics of adsorption

The following three kinetic models, namely the pseudo-first-order model (Eq. (3)) [22], pseudo-second-order model (Eq. (4)) [23], and intra-particle diffusion model (Eq. (5)) [24] were applied to fitting the experimental data at initial Cu^{2+} concentration of 100 mg/L and ceramsite dosage of 0.5 g. The fitting results are shown in Fig. 8, Tables 2 and 3.

$$\ln(Q_e - Q_t) = \ln Q_e - K_1 t \quad (3)$$

where K_1 is the rate constant of the pseudo-first-order adsorption.

$$\frac{t}{Q_t} = \frac{1}{K_2 Q_e^2} + \frac{t}{Q_e} \quad (4)$$

where K_2 is the rate constant of the pseudo-second-order adsorption.

$$Q_t = K_p t^{1/2} + c \quad (5)$$

where K_p is the intra-particle diffusion rate constant; c is a constant.

According to Fig. 8 and Table 2, the linear correlation coefficients of R^2 for the pseudo-first-order model and the pseudo-second-order model both are very high. The equilibrium adsorption capacity (Q_{e2}) through pseudo-second-order is 9.644 mg/g, which is very close to the experimental data mentioned above ($Q_e=9.421$ mg/g). Results indicate that the kinetics of Cu^{2+} adsorption by the ceramsite fits the pseudo-second-order model well. Accordingly, it can be deduced that the adsorption of Cu^{2+} by the ceramsite is kinetically controlled by external film diffusion, surface adsorption and intra-particle diffusion.

According to Fig. 8 and Table 3, the fitting line for total stage of intra-particle diffusion does not intersect the Y-axis at zero point, indicating that the adsorption is controlled by more than two factors [25]. From Table 3, the diffusion coefficient for the first diffusion stage ($K_p=0.21933$) is far greater than that of the second stage

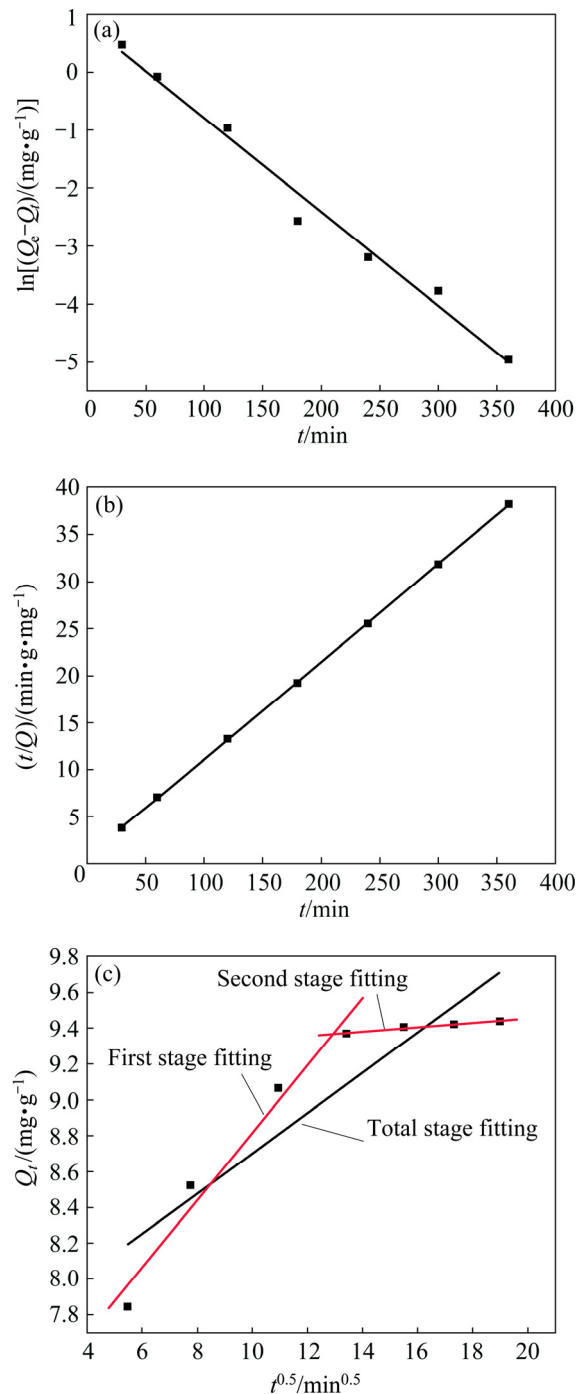


Fig. 8 Kinetic fitting plots of Cu^{2+} adsorption by ceramsite with pseudo-first-order model (a), pseudo-second-order model (b), and intra-particle diffusion model (c)

($K_p=0.01168$). This is because in the first stage, the ceramsite contains plenty active sites to adsorb Cu^{2+} . The adsorption is mainly controlled by diffusion factor. In the second stage of adsorption, the active sites are gradually occupied by Cu^{2+} , leading to adsorption performance decreasing. Consequently, the adsorption is mainly controlled by surface adsorption and other factors. Therefore, during the initial stage of treating real

Table 2 Kinetic fitting results for Cu^{2+} adsorption by ceramsite ($T=303\text{ K}$)

Pseudo-first-order model			Pseudo-second-order model		
$Q_{e1,cal}$	K_1	R^2	$Q_{e2,cal}$	K_2	R^2
2.315	0.0163	0.9819	9.644	0.0148	0.9999

Table 3 Kinetic fitting results for Cu^{2+} adsorption by ceramsite with intra-particle diffusion model ($T=303\text{ K}$)

Intra-particle diffusion stage	Fitting equation	K_p	c	R^2
Total stage	$y=0.10097t^{1/2}+7.68592$	0.10097	7.68592	0.7825
First stage	$y=0.21933t^{1/2}+6.71006$	0.21933	6.71006	0.9465
Second stage	$y=0.01168t^{1/2}+9.21611$	0.01168	9.21611	0.9737

wastewater with the tungsten residue-based ceramsite, the removal of heavy metal ions can be improved through enhancing agitation of the wastewater solution.

3.4 Reusability of porous ceramsite

Recycling of adsorbents is of especial importance. In the present study, we used the acid desorption for recycling. After three cycles of adsorption and desorption, the adsorption capacity of the ceramsite for Cu^{2+} still kept a relatively high value of about 8.215 mg/g, showing the good reusability. After six cycles of adsorption and desorption, the adsorption capacity decreased sharply to about 4.556 mg/g, suggesting that the ceramsite was no longer suitable for adsorption. But it still can be used as a building material in the point of overall reusability.

4 Conclusions

1) The surface of the ceramsite prepared with tungsten residue and diatomite is rough and porous with lots of perforative pores. The ceramsite possesses high specific surface area and one of its main component is MnFe_2O_4 , which is helpful for adsorption.

2) The adsorption capacity of Cu^{2+} by the ceramsite reaches 9.421 mg/g with copper removal efficiency of 94.21% under the conditions of 303 K, the initial Cu^{2+} concentration of 100 mg/L, the ceramsite dosage of 0.5 g and 300 min. With increase of ceramsite dosage, the total adsorption amount of Cu^{2+} increases, while the adsorption capacity decreases. The adsorption capacity increases with the increase of initial pH of the solution. The ceramsite can be applied as an effective adsorbent for heavy metal-containing wastewater treatment. And the absorption time can be determined as 300 min.

3) The isothermal adsorption of Cu^{2+} by the ceramsite fits the Freundlich model better. The adsorption mainly occurs on a heterogeneous surface and is a favorable process. The adsorption process closely follows the pseudo-second kinetic equation, and is kinetically controlled by liquid film diffusion, surface

adsorption and intra-particle diffusion. In initial stage of wastewater treatment, the adsorption process should be controlled mainly by diffusion. The removal of Cu^{2+} from real wastewater can be improved through enhancing agitation.

References

- [1] SONG Y X, CHAI L Y, TANG C J, XIAO R, LI B R, WU D, MIN X B. Influence of ZnO nanoparticles on anammox granules: The inhibition kinetics and mechanism analysis by batch assays [J]. *Biochemical Engineering Journal*, 2018, 133: 122–129.
- [2] TANG Chong-jian, DUAN Cheng-shan, YU Cheng, SONG Yu-xia, CHAI Li-yuan, XIAO Rui-yang, WEI Zong-su, MIN Xiao-Bo. Removal of nitrogen from wastewaters by anaerobic ammonium oxidation (ANAMMOX) using granules in upflow reactors [J]. *Environmental Chemistry Letters*, 2017, 15(2): 311–328.
- [3] FREITAS E D D, ALMEIDA H J D, VIEIRA M G A. Binary adsorption of zinc and copper on expanded vermiculite using a fixed bed column [J]. *Applied Clay Science*, 2017, 146(15): 503–509.
- [4] CHAI Li-yuan, PENG Cong, MIN Xiao-bo, TANG Chong-jian, SONG Yu-xia, ZHANG Yang, ZHANG Jing, ALI M. Two-sectional struvite formation process for enhanced treatment of copper-ammonia complex wastewater [J]. *Transactions of Nonferrous Metals Society of China*, 2017, 27: 457–466.
- [5] CHAI L, WANG Y, ZHAO N, YANG W, YOU X. Sulfate-doped $\text{Fe}_3\text{O}_4/\text{Al}_2\text{O}_3$ nanoparticles as a novel adsorbent for fluoride removal from drinking water [J]. *Water Research*, 2013, 47: 4040–4049.
- [6] CHEN Yong-gui, YE Wei-min, YANG Xiao-min, DENG Fei-yue, HE Yong. Effect of contact time, pH and ionic strength on Cd (II) adsorption from aqueous solution onto bentonite from Gaomiaozhi, China [J]. *Environmental Earth Sciences*, 2011, 64(2): 329–336.
- [7] XING Yi, TIAN Xing-qiang, LU Shao-yong, HU Wei-zheng, LI Ji-sheng, LI Ke, JIA Jian-li. Characteristics of phosphorus adsorption by ceramsite in vertical subsurface flow constructed wetlands treating lake water [J]. *Chinese Journal of Environmental Engineering*, 2014, 11(8): 4820–4823. (in Chinese)
- [8] WANG Jian-long, ZHAO Yuan-ling, ZHANG Ping-ping, YANG Li-qiong, XU Huaiao, XI Guang-peng. Adsorption characteristics of a novel ceramsite for heavy metal removal from stormwater runoff [J]. *Chinese Journal of Chemical Engineering*, 2018, 26(1): 96–103.
- [9] JI Guo-dong, ZHOU You, TONG Jing-jing. Nitrogen and phosphorus adsorption behavior of ceramsite material made from coal ash and metallic iron [J]. *Environmental Engineering Science*, 2010, 27(10): 871–878.
- [10] LIU Jun-zhe, LIU Rui, HE Zhi-min, BA Ming-fang, LI Yu-shun. Preparation and microstructure of green ceramsite made from sewage

- sludge [J]. Journal of Wuhan University of Technology (Materials Science Edition), 2012, 27(1): 149–153.
- [11] YANG Jin-zhong, GAO He-feng, WANG Ning, CHEN Lin, WANG Jian-yuan, YANG Yu-fei. Research on polluting characteristic of tungsten residue from ammonium paratungstate (APT) [J]. Journal of Environmental Engineering Technology, 2015, 5(6): 525–530. (in Chinese)
- [12] CJ/T 299–2008, Artificial ceramsite filter material for water treatment [S]. (in Chinese)
- [13] HJ/T299–2007, Solid waste-Extraction procedure for leaching toxicity- Sulphuric acid & nitric acid method [S]. (in Chinese)
- [14] GB 5085.3–2007 Identification standards for hazardous wastes-Identification for extraction toxicity [S]. (in Chinese)
- [15] PODDER M S, MAJUMDER C B. Sequestering of As(III) and As(V) from wastewater using a novel Neem leaves/MnFe₂O₄ composite biosorbent [J]. International Journal of Phytoremediation, 2016, 18(12): 1237–1257.
- [16] XU Nai-cen, SHEN Jia-lin, LUO Hong-yu. Analysis for crystallinity of kaolinites by X-ray diffractometer and infrared spectroscopy [J]. Resources Survey and Environment, 2014, 35(2): 152–156. (in Chinese)
- [17] JING Qing-xiu, CHAI Li-yuan, HUANG Xiao-dong, TANG Chong-jian, GUO Huan, WANG Wei. Behavior of ammonium adsorption by clay mineral halloysite [J]. Transactions of Nonferrous Metals Society of China, 2017, 27(7): 1627–1635.
- [18] MIRZAYI B, NEMATOLLAHAZADEH A, SERAJ S. Synthesis and characterization of magnetic maghemite/catecholamine core/shell nanoparticles [J]. Powder Technology, 2015, 270(4): 185–191.
- [19] XIA Lu, HU Yi-xu, ZHANG Bo-han. Kinetics and equilibrium adsorption of copper(II) and nickel(II) ions from aqueous solution using sawdust xanthate modified with ethanediamine [J]. Transactions of Nonferrous Metals Society of China, 2014, 24: 868–875.
- [20] KHOSRAVI P, SHIRVANI M, BAKHTIARY S, SHARIATMADARI H. Energetic and entropic features of Cu(II) sorption equilibria on fibrous clay minerals [J]. Water Air & Soil Pollution, 2016, 227(9): 354–365.
- [21] KUMAR M, TAMILARASAN R. Kinetics, equilibrium data and modeling studies for the sorption of chromium by prosopis juliflora bark carbon [J]. Arabian Journal of Chemistry, 2017, 10 (S2): s1567–s1577.
- [22] FREITAS G R, VIEIRA M G A, SILVA M G C. Kinetic adsorption of copper ions by the residue of alginate extraction from the seaweed sargassum filipendula [J]. Chemical Engineering Transactions, 2017, 57: 655–660.
- [23] IVANETS A I, SHASHKOVA I L, KITIKOVA N V, MOROZOV Y. The kinetic studies of the cobalt ion removal from aqueous solutions by dolomite-based sorbent [J]. International Journal of Environmental Science and Technology, 2016, 13(11): 2561–2568.
- [24] BERHANE T M, LEVY J, KREKELER M P S, DANIELSON N D. Kinetic sorption of contaminants of emerging concern by a palygorskite–montmorillonite filter medium [J]. Chemosphere, 2017, 176: 231–242.
- [25] NASSA M M. Intraparticle diffusion of basic red and basic yellow dyes on palm fruit bunch [J]. Water Science and Technology, 1999, 40(7): 133–139.

硅藻土–钨渣基陶粒对废水溶液中铜离子的吸附

靖青秀^{1,2}, 王云燕¹, 柴立元¹, 唐崇俭¹, 黄晓东², 郭欢², 王魏², 游威²

1. 中南大学 冶金与环境学院, 长沙 410083;

2. 江西理工大学 冶金与化学工程学院, 赣州 341000

摘要: 为了在中国南方有色矿冶区同时实现工业钨渣的资源化利用和重金属废水的处理, 以钨渣和硅藻土为主要原料制备一种新型陶粒, 对其与溶液中重金属 Cu²⁺的吸附规律进行研究。结果表明: 新制备的近球形陶粒表面粗糙多孔, 内部有许多贯穿性孔道与外部相连通; 陶粒的主要物相组成含有 MnFe₂O₄。在 303 K、铜离子初始浓度 100 mg/L、陶粒投加量 0.5 g 和 300 min 条件下, 陶粒对 Cu²⁺的吸附量为 9.421 mg/g, 吸附去除率达 94.21%。随着陶粒投加量的增大, 其对溶液中 Cu²⁺的总吸附量增大, 单位吸附量降低; 陶粒对 Cu²⁺的吸附量随试验 pH 值的增大而增大。陶粒对 Cu²⁺的等温吸附更符合 Freundlich 模型, 吸附主要发生在非均质表面, 为优惠吸附; 陶粒对铜离子的吸附动力学符合准二级动力学方程, 吸附过程主要受液膜扩散、表面吸附以及颗粒内扩散因素控制。对于实际重金属废水的处理, 陶粒对重金属离子的吸附初始阶段受扩散控制, 此时, 可通过加强搅拌的方式提高 Cu²⁺的去除率。

关键词: 钨渣; 陶粒; 重金属废水; Cu²⁺; 吸附

(Edited by Xiang-qun LI)